Development of a Motor Controller for the São Rafael 03 Boat's Motors

Tiago Ferreira
tiagoamferreira@tecnico.ulisboa.pt

Instituto Superior Técnico, Universidade de Lisboa, Portugal

November 2021

Abstract

Técnico Solar Boat (TSB) is a team who competes in international solar powered boat championships, by means of their vessels of the São Rafael line, currently in it's third generation, São Rafael 03 or SR03 for short. As means to stimulate learning in the various subjects, and proving itself in various fields, the team desires to produce more of the boat's core components in-house, having decided to begin development on a self-made motor controller, whose hardware's design is the subject of this thesis.

A decision had already been made to build a small scale prototype first, whose development had been started before, as such this work begins with finalizing it's design and building the first prototype. An early version of a control algorithm was also developed for the prototype's testing phase, which revealed some flaws in it's design. Nonetheless, lessons were learnt and the full-size motor controller's design was initiated, starting with estimating the power losses of several available transistor and gate driver choices available on the market, followed by designing the remaining sub-circuits needed for the motor controller, whose power stage is based on a three-phase inverter, galvanically isolated from the control circuitry. The PCB was then laid-out, which required additional laser-cut copper bus-bars to be added, so as to be able to handle the large currents. These were followed with designing a custom PCB-Liquid cooler, as no commercial solutions were available, and a plastic cover to protect the board against electrical risks and mechanical damage.

Keywords: Electric Vehicles, Electronic Speed Controller (ESC), Brushless Direct Current (BLDC) Motor, Three-Phase Inverter, Técnico Solar Boat

I. Introduction

With a growing public concern about the usage of fossil fuels as energy source for vehicles, leading to an exaggerated greenhouse effect and consequential increase in global warming, the demand for environmentally friendly means of transportation is increasing steadily. Such demand calls for innovation in the area, leading several entities to host events promoting the development of such solutions, as well as the involvement of the younger generations in the area. TSB participates in some of these events, with special emphasis on *Yacht Club du Monaco's* Monaco Solar & Energy Boat Challenge, whose rules are used as guidelines for most of their boats' development.

Of these rules, the most important for this work's development is the maximum battery voltage of $48V$, maximum battery energy of $1500W.h$, a limited solar panel area, and thus power and the need for all electronics to sit in watertight compartments. The competitions are composed of several races, some of which evaluate performance while others put an emphasis on overall efficiency. These two different demands were covered by TSB by means of a dual motor system, whereby both a $5kW$ and a $10kW$ are used simultaneously, using the smaller, more efficient motor exclusively when efficiency is more valuable than performance, and both when it's the performance that's needed.

After many failed controllers, TSB eventually settled with the usage of VESC 75/300 ESC's by Trampa Boards, partly open source commercial controllers which have, for the most part, satisfied their needs. However, they too have shown difficulties in handling the high currents needed for the high power motor, even though they are within their rated current and custom water-cooling heat sinks have been added. Additionally, problems have been discovered arising from the usage of 2 units on the same circuits, leading to the destruction of several micro-controllers in the process. These were later discovered to be ground loops, resulting in high currents on the data lines which required some non-optimal workarounds. This led galvanic

isolation between the power electronics side of the circuit and it's control counterpart to be a highly desirable feature, as it would lead to the complete elimination of such possibility.

The current motors installed in SR03 have 10 pole pairs and have a top speed of around $10000rpm$, resulting in high frequency input signals, which by themselves mean an even higher switching frequency is required. Combining this high switching frequency with the high currents at stake and the controller's enclosed compartment results in a high efficiency not only being desired, but required, as excess heat is not easily evacuated.

II. BLDC Motor Control Fundamentals

A BLDC motor is composed of a rotor and stator. The stator contains a set of electromagnetic poles in it's stator, equally distributed by it's 3 phases which are usually star connected, with a non accessible common point, and wired in such a way that when any two phases get energized both a magnetic north and south poles appear on the stator's magnetic field. The rotor, however, usually contains permanent magnets, in alternate polarities, whose amount dictates how many pole pairs the motor has, half of the total number of magnets. In figure 1, showing the construction of the motor used during the initial tests, it's clearly visible not only the 12 electromagnetic poles composing the stator on the left, but also the 14 permanent magnets on the rotor on the right, which make it a 7 pole pair BLDC motor. This specific motor has the rotor spinning around and outside the stator, in a setup called Outrunner.

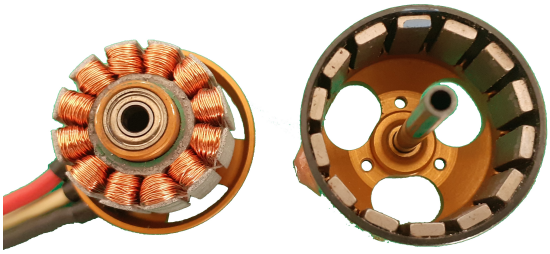

Figure 1: BLDC stator (left) and rotor (right).

II.A. A. *Trapezoidal Control*

The simplest control algorithm, and the most commonly used especially in small motors, is the trapezoidal control. In figure 2a a schematic representation of a BLDC motor is depicted, with two phases, B and C, energized. These phases produce two magnetic poles, a north and a south respectively, acting simultaneously on the rotor, which has a south pole between them. Phase C's south pole repels the rotor's south pole, while phase B's North pole attracts it, generating torque. However, when the rotor's south pole reaches phase B, the rotor position depicted in figure 2b, the system will reach equilibrium. However, if the energized phases become the ones depicted there, two new forces will appear to the energized poles, and torque will be reestablished. If the phases get switched as depicted in figure 2, where each position is called a sector, in sync with the rotor, a complete cycle will be established, and the motor will spin, producing useful torque.

This is the working of the trapezoidal control algorithm, which leaves a problem to be solved: the detection of the rotor position. There are two main solutions in current use, the addition of a sensor capable of detecting when the phases need to be switched, whose usage is refered to as sensored trapezoidal control, or the detection of zero crossings on the open phase, the sensorless trapezoidal control approach.

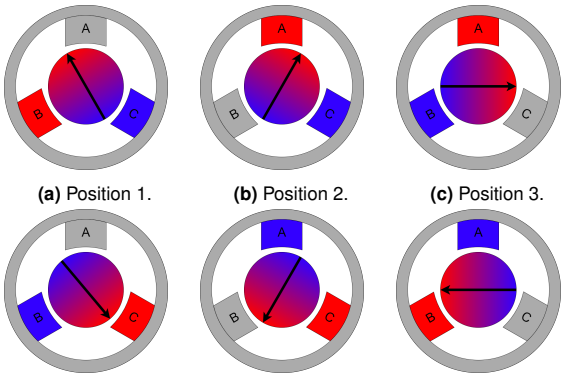

(a) Position 1. **(b)** Position 2. **(c)** Position 3.

(d) Position 4. **(e)** Position 5. **(f)** Position 6.

Figure 2: Trapezoidal control sequence.

II.B. *Sensorless Trapezoidal Control*

A permanent magnet BLDC motor produces an Electromotive Force while rotating, as the rotor's magnetic field closes through the stator's poles, and since the field's polarity reverses during the rotation, there must be a changing magnetic flux going through each stator pole, which leads to an induced EMF in the coils, including any inactive phase. The resulting back-emf shape is represented in figure 3, whose trapezoidal shape gives this control algorithm it's name. Note, in figure 2 that a rotor's pole always aligns with the inactive phase exactly in the middle of each step. This leads to an increase of magnetic flux going through the stator pole in the first half of the step, and a decrease in the other half, which in turn means there is a point exactly in the middle of each step where the derivative of the magnetic flux going through the inactive phase's pole is zero, which in turn means the back-EMF in that phase will be zero in

that instant.

Using a simple circuit it's possible to detect the zero crossing on the open phase's back-EMF, which dictates the step's midpoint. Since the step was generated by a micro-controller, it's possible to record when it begun, and given it's midpoint it's easy to predict when it will end, simply by measuring the time interval from the step's beginning to the zero crossing and waiting an equal amount from this zero crossing, with just a slight correction needed if the motor's angular acceleration is not null. This is the basis on which the sensorless trapezoidal control works, by timing the step commutations using the zero crossings, a simple algorithm which only requires 3 simple zero crossing detection circuits, one per phase.

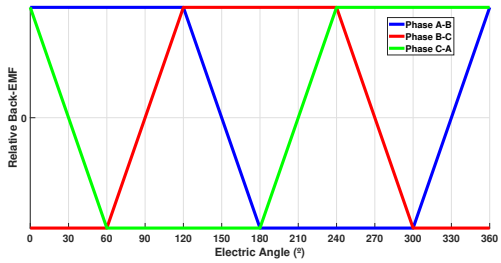

Figure 3: BLDC motor's Back-EMF shape.

Despite being a simple control algorithm, the trapezoidal control possesses a major issue: it produces torque ripple. This is due to 2 reasons, the first is the motor's inductance, which makes the phase commutations non-instantaneous, as the current varies exponentially. Since the current and the developed magnetic forces are proportional, the torque will experience variations during commutations. The second, and most important reason, is the fact that the developed torque is not constant, as the angle between the rotor's magnetic field and the stator's magnetic field varies between $60°$ and $120°$ during a step. Through force decomposition the rotor will experience a tangential force, which generates torque, and a normal force, which deforms the rotor and produces no useful work. The tangential force is maximum when the rotor's and stator's magnetic fields are perpendicular to each other, as it varies with it's angle's sine. Simultaneously, the normal force will be null, as it varies with the angle's cosine. This results in the torque curve shown in Figure 4, where the phase current shape is also visible. This torque ripple can be problematic if the load has a small moment of inertia, as it won't absorb it and will oscillate, causing noise and power losses, and thus, less efficiency.

This problem can only be solved by maintaining the angle between both magnetic fields constant, preferably at $90°$ in order to maximize the torque, which is what the Field Oriented Control Algorithm attempts to do.

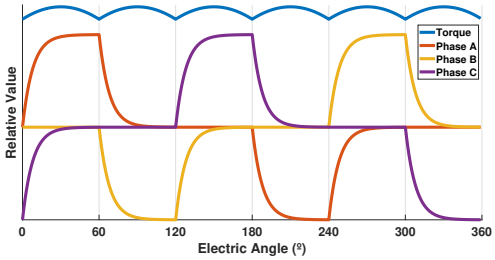

Figure 4: Trapezoidal Control Current and Torque Curve Shapes.

II.C. Field Oriented Control

Powering two of the three phases it's possible to achieve a magnetic field on the stator with 6 different directions, which will not be perpendicular to the rotor's magnetic field for most of the time. However, if the third phase is also energized, two fields will be formed simultaneously, whose combination is actually a single magnetic field with any direction inside the rotor (Figure 5). Thus, by controlling the current in each phase it is possible to obtain a rotating magnetic field in the stator, perpendicular to the rotor's magnetic field at all times, with maximum, ripple free torque during the entire revolution.

The stator magnetic field is the sum of three magnetic fields, one per phase, whose strengths are directly proportional to their respective phase currents. However, only two components are needed to describe it, since it can be assumed constant throughout the entire stator's length, and thus represented by it's cross section. Using the Park transform the resulting magnetic field becomes represented by only 2 currents, which rotate with the rotor. Since these currents rotate synchronously with the rotor, they are stationary from it's point of view, so using the Clark transform they become the direct and quadrature, i_d and i_q, currents, which represent the current, and thus magnetic field intensity normal and tangential, respectively, to the rotor as DC values. These values are easily controlled with PID loops, and backwards Clark and Park transforms can be applied to obtain the desired phase voltages the controller shall apply to the motor. These transforms employ trigonometric functions, and are thus computationally demanding.

These transforms require the rotor angle as input, which can be measured via a sensor capable of sufficient resolution at the high speeds the motor will be spinning, resulting in the Sensored FOC motor control algorithm, or can be estimated using a mathematical model of the system, estimating the phase currents and comparing with their actual values. This is a computationally intensive

task whose functioning is beyond the scope of this work, and results in the Sensorless FOC algorithm which is what the final product is supposed to run.

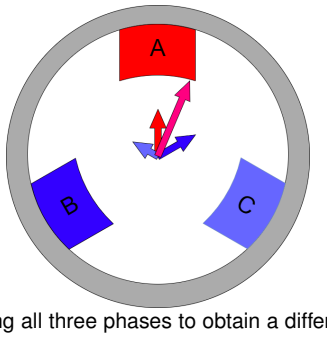

Figure 5: Using all three phases to obtain a different magnetic field direction.

II.D. Hardware requirements.

The previous theoretical basis has shown the needs each control algorithm requires. Since all three motor phases need to be switched either to the supply voltage or ground, a three-phase inverter is needed, becoming the basis of the controller. The easier control algorithms are the ones who employ sensors, thus there should be a provision for their use, not only to offer the capability of trying sensored algorithms, but also to make their sensorless counterpart's development easier. Finally, the sensorless trapezoidal control algorithm requires 3 zero crossing detection circuits, and the sensorless FOC the instantaneous current in each of the phases, as well as a powerful microcontroller.

III. Building the TSB Motorcontroller Initial Prototype

III.A. Prototype Design Finishing

The team had already taken the first steps in designing their own motor controller, having laid the foundations for a small scale prototype, the TSB Motorcontroller. It's design was close to being finished, composed of two boards, one with the three phase inverter and another with the remaining circuitry, interconnected by a large pin header. The idea behind was to easily replace the high power electronics in case of damage, retaining the logic circuitry.

The design was based around a three-phase inverter, composed of 6 MOSFETs which were controlled by a Texas Instruments DRV8302 Gate Driver chip, which also contained the current measuring capability to read two current shunts, and was ran by a Teensy 3.2 development board. Finally there were two power supplies generating a $3.3V$ and $5V$ rails and some external communication circuitry. A design error was, however, discovered: the analog comparators built into the Teensy 3.2 micro-controller, needed for the zero-crossing detection, used pins needed for the critical CAN-BUS communication.

Thus, a zero crossing detection circuit had to be developed, whose schematic is shown in figure 6. The component selection was rather important, as the analog comparator does not tolerate large negative voltages at it's input, which is the reason a diode was added, limiting the voltage in the negative parts of the input signal. However, when reverse biased the voltage across it is relatively small, giving it's junction capacitance a significative impact on the circuit's delay. Relatively low value resistors had to be used in order to improve it, and a fast diode with low junction capacitance had to be picked.

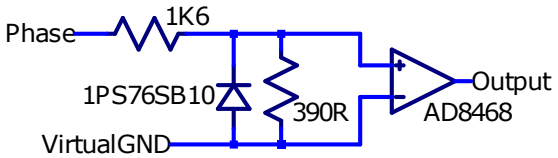

Figure 6: Single phase zero-cross detection circuit schematic.

A new PCB was designed, containing the newly developed zero-cross detection circuitry, as well as new MOSFETs and a ground current measuring shunt resistor, as it's possible to obtain all three phase currents from this single shunt, and such capability had to be accounted for.

III.B. Prototype programming.

As a way to test the prototype's functioning, a simple trapezoidal control algorithm was developed, along with the auxiliary functions needed for the board's functioning. These include the current measurement and calibration and external PC communications, along with a simple Graphical User Interface to send commands and display the retrieved data.

The control algorithm contains 2 step defining functions, one which selects the next sector, using time measurements from the zero-cross detections, and another which chooses between two states for that sector, one with power applied to it's coils and another which short-circuits them. These two states provide the means to generate a PWM signal which can be used to regulate the phase voltages, and thus currents, who finally provide the means to control the motor's speed. The PWM signal's duty cycle was controlled first with a hysteresis or bang-bang controller, and later updated to a PID loop. Finally, there is a function responsible for correcting the sector duration based on detected acceleration.

III.C. Prototype Testing.

Both of the prototype's PCBs were built (Figure 7) and some tests were performed. The initial test replaced the motor with 3 T10 $24V$ light bulbs wired in star configuration, and showed the circuit was indeed capable of flashing them as desired.

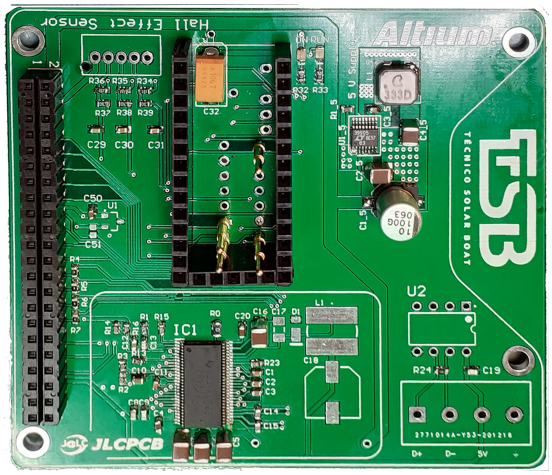

(a) Logic PCB.

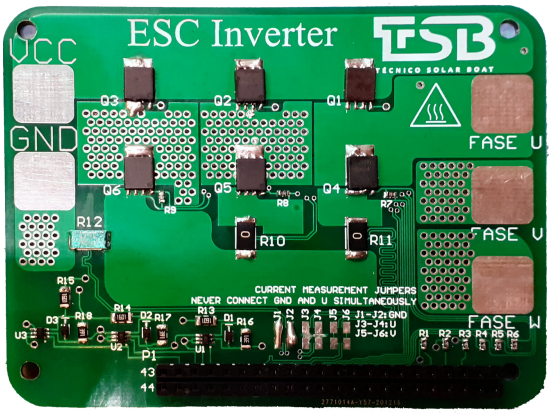

(b) Inverter PCB.

Figure 7: TSB MotorController's complete PCBs.

Having proven the three-phase inverter was working, the bulbs were replaced with the motor from Figure 1 and testing continued, making the motor spin, although in a jerky motion. It was soon noticed an abnormal heating of the High Side MOSFETs, in comparison with the Low Side ones, who remained cool. Some probing revealed the Bootstrapping circuit was not working as intended, providing too low of a voltage at the High Side MOSFETs' gates to drive them into saturation. As a result, they were operating in their linear region and producing excessive losses.

This was figured to be caused by a mistake in the design stage, where 3 connections from the Gate Driver to each High Side MOSFET Source were forgotten, and since they were the reference for the gate voltage in these MOSFETs the IC was unable to properly apply it, thus being incapable of properly driving them. Some Blue Wires were added, in an attempt to correct the problem, but a soldering accident damaged the Gate Driver IC, which had to be replaced. The circuit was first powered on without the Blue Wires, and the previous behaviour was expected. However, the new Gate Driver continuously reported an overcurrent situation instead. It was theorized to be due to measuring floating V_{ds} voltages due to a lack of proper connection to the Source, so the Blue Wires were again added and the circuit resumed it's previous behaviour.

The Gate Driver was found to be issuing an alert, as an undervoltage alarm was being triggered. It was found to be phase W's bootstrap capacitor voltage, which was dropping rather quickly upon turning it's MOSFET on, and a short in the IC's pins was discovered. This was assumed to be caused by another probing accident, and thus the chip was replaced again. The new Gate Driver IC promptly spun the motor, but after turning it off it failed to ever spin it again. The same short circuit was again discovered, proving it had not been caused by bad probing. After reaching out to the manufacturer it was discovered the missing connections had to be dealt with special care, as there were large current spikes going through them. As such, they should be as short as possible, ideally treating them as a differential pair, with as little inductance as possible. The idea of separating the Gate Driver IC onto it's separate board was thus proven bad, and the added Blue Wires incapable of properly replacing the missing tracks. In a last resort attempt, the gate resistances were doubled, in the hope of decreasing these current spikes and thus protecting the IC, with no success.

By this time it was also noted the firmware was running far too slowly, at around 1500 cycles per second. Some tweaks were made which increased it's speed to around 4000 cycles per second, which is still insufficient. Thus, a more optimized code was needed, or, a faster processor.

This prototype was thus abandoned, and work begun on the full size controller, after learning how much care should be taken while routing the Gate Driver connections, as well as the gate circuit's components, which should be placed as close as possible to the transistor.

IV. Full Size Motor Controller

IV.A. Design Criteria.

The full-size controller must be able to handle the larger of the SR03's motors, so as to be able to handle either of them. This is a $48V$ $10kW$ 10 pole pair motor capable of reaching around $10000rpm$. This equates to a DC bus current of around $230A$

if a 90% efficiency is assumed and a phase frequency of about $1.7kHz$. Since the current commercial controller is rated for $300A$ this figure was used for this controller's development, and since the switching frequency should be much higher than the phase frequency a $17kHz$ figure was used as a starting point. A few other design criteria were chosen as well, starting with the galvanic isolation between the high power and control electronics, which should prevent any ground loop problems. The power electronics shall be watercooled, as this is the only sensible way to extract high amounts of heat losses from the watertight compartment the controller will be installed in, and is in fact the current cooling solution. The current Teensy 3.2 shall be replaced by a Teensy 4.0, which has a similar cost but is far more capable and finally, components from the team's sponsors should be preferred.

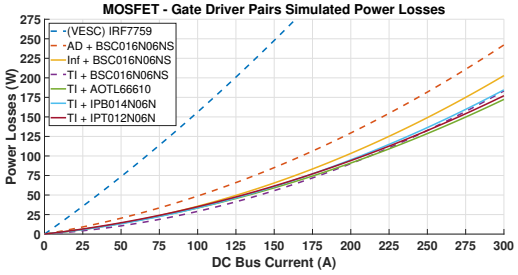

Figure 8: Simulated power losses for the top performing combos.

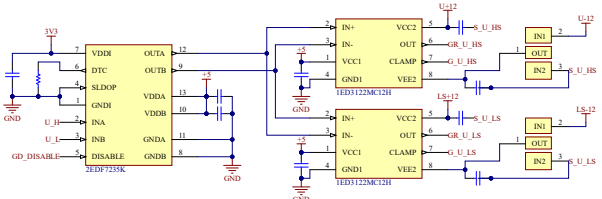

Figure 9: Half-Bridge Gate Driver Circuit Topology.

IV.B. MOSFET and Gate Driver Choice.

There are several power transistor technologies on the market, however, most of them are meant to be used with high voltages, being based on the bipolar transistor. This leads to a considerable voltage drop across them when compared to the battery's $48V$, of around $2V$. Thus the usage of regular N-Channel MOSFETs was decided. These devices will be paired with Gate Driver IC's, so their choice shall be made conjointly.

3 Gate Driver IC's were selected, Analog Devices ADuM4137, Infineon 1ED3122MC12H and Texas Instruments UCC5870-Q1. Several MOSFETs were also chosen, whose selection was made considering a total $R_{DS(on)}$ lower than the current controller's, accounting for any paralleling up to 3 devices, so as to limit the board area, as well as a low gate capacitance, sufficient current carrying capability and fast enough rise and fall times, which shall reduce the switching losses. These MOSFETs were all rated for $60V$, which despite offering a small safety margin, offer considerably smaller $R_{DS(on)}$ than their higher voltage counterparts, thus improving the overall efficiency.

The power of both conduction losses and switching losses was computed for several situations and Gate Driver-MOSFET combos, with the top performers being selected and faced off, resulting in Figure 8's plot, where the current controller's combination also figures. It can be seen that all the selected combos should perform better than the current controller, which should help reducing overheating, and that the Analog Devices Gate Driver performs slightly worse than both the Infineon and Texas Instruments options. The TI gets it's performance from it's very high output current of $15A$, while the Infineon and AD ones only output $10A$ and $6A$, respectively. This leads to very short rise and fall times, which could lead to excessive noise, and thus not be practical in reality. Thus, the Infineon Gate Driver was chosen, as it performs almost as well as the TI options, but it's a sponsored product and has a far simpler implementation. It's paired with 3 BSC016N06NS paralleled MOSFETs, also from Infineon, and a freewheeling diode for extra protection and quicker turn-off times. All these Gate Drivers are single channel, thus 6 of them will be needed, but allow for much shorter connections between the IC and the MOSFETs.

IV.C. Circuit Topology.

Since the chosen Gate Driver has no built-in capability to generate dead time, which delays the turn-on to prevent current shoot-through, a different than usual topology was chosen, with an Infineon 2EDF7235K Half-Bridge Gate Driver Controlling the two single-channel Gate Drivers in each Half-Bridge (Figure 9), which not only allows for a Hardware based dead time, but also adds another layer of security against an accidental turn on of both sides of the Half-Bridge. There will be no Bootstrapping circuit, instead the Gate Drivers will be powered from isolated DC-DC converters from Traco Power, and the possibility for both Unipolar and Bipolar driving of the MOSFETs was provisioned, as well as a High Side Switch capable of turning the DC-DC converters off when not needed. Attached to each MOSFET gate there is a gate charge and discharge circuit (Figure 10) which allows for separate charge and discharge resistances, as well as the usage of the Gate Driver's Miller Clamp and contains a provision for a ferrite bead in case extra noise reduction is needed.

The current measuring will be made using a shunt resistor per phase, as other technologies

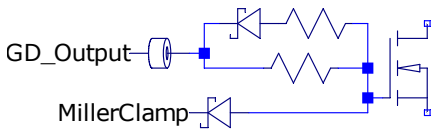

Figure 10: Gate Charging and Discharging Circuit.

such as current transformers and hall effect sensors do not have as much bandwidth, while at the same time being more expensive, complicated and taking up more board space. While it is possible to measure the currents with a single shunt on the DC bus, such option was not tested on the previous prototype, so it was not implemented on this version. The 3 shunt design offers extra reliability, as measurements can be compared between the shunts.

These will be read using isolated Sigma-Delta Modulators from Analog Devices, model ADuM7704. The same family offers the ADuM7703, whose only difference is the greater input range, so one of them will be used along a resistive divider to measure the input voltage. These modulators will produce a signal which will be read inside an AMC1210 digital filter from Texas Instruments, producing readings available to the microcontroller through serial interface. This option was taken instead of the Teensy's on-board DSP as it should be easier to set up, while offloading some processing power from it. Finally, this is a very affordable IC, which further solidified the choice.

As far as the Teensy goes, it's 4.0 version was chosen to replace the previously used 3.2, as it offers hardware based floating point math, which should make a significant difference in the processing of algorithms such as sensorless FOC which rely heavily on it, and runs at a nearly ten fold speed, while costing the same. The only drawback is it's $3.3V$ only logic level.

Additionally, the zero-cross detection circuit had to be modified in order to work with the galvanic isolation (Figure 11). This meant reading the phase, and not the virtual Ground, resistors of the dividers. This means they can be powered from the isolated DC-DC converters which feed the Gate Drivers, using an LDO without exceeding their common-mode input voltage. Since the comparators are not galvanically isolated, a digital isolator model ADuM110N from Analog Devices was attached to each of them, in order to send the signal across the isolation barrier.

Some input protection was added with a fuse and an inversely polarized diode, which should conduct in case of wrong polarity, shorting out the supply and blowing the fuse, hopefully protecting the circuit. Finally, a CAN-BUS transceiver was added, as well as an Analog Devices LTC2984 IC, which is capable of reading several sensors, such

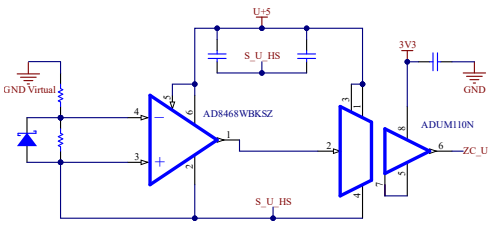

Figure 11: The new zero cross detection circuit.

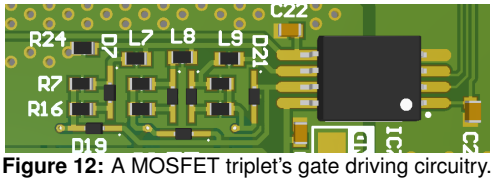

Figure 12: A MOSFET triplet's gate driving circuitry.

as thermistors. Thus, 6 thermistors were added, one to each MOSFET triplet, as well as a connector which allows more thermistors to be externally connected, allowing the measurement of, for example, the motor and coolant temperatures. All the extra unused pins in the Teensy were routed into a pin header, and special care was taken to have them include one of each available communication protocol, allowing for the use of external hardware such as sensors, or even actuators, which could turn the controller into a multi-function board when installed on the boat.

IV.D. PCB Design.

There were two main layout problems to consider. The first was keeping all the gate driving circuitry confined, so as to avoid the fatal flaw seen on the first prototype, and the second was dealing with the high currents and heat generated.

The first problem was dealt with by carefully laying out the gate driving circuitry in such a way that for each MOSFET triplet the whole circuit takes just $3cm^2$ of board space (Figure 12), and is installed immediately underneath the transistors, leading to very short paths and small loop areas.

The second problem was sorted by installing the MOSFETs and Diodes in a linear arrangement, with laser cut busbars soldered in between, forming not only the high current path but also a path for the heat to dissipate from the MOSFETs through them and into the heat sink which is installed over both the busbars and the MOSFETs, inside the channel formed by the former (Figure 14a). This makes for a compact design with very little reliance on the thin PCB copper for current handling, whilst also providing some solid mounting tabs for the cable lugs to bolt on to. The busbars originally had the tabs on their ends (Figure 14a), but had to be modified to avoid interference with the water inlet (Figure 14b). Additional busbars were designed for the motor coil terminals, which allow for the connection using cable lugs in a similar fashion. All

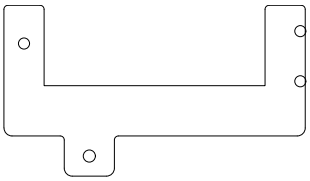

Figure 13: Battery Busbar Cutout.

these busbars are simple to manufacture, with only 3 profiles needing to be cut, of which 2 require a simple bend. The battery busbars, in fact, are symmetrical, and only require the same profile to be bent either to the right or to the left, thus decreasing the total parts count (Figure 13).

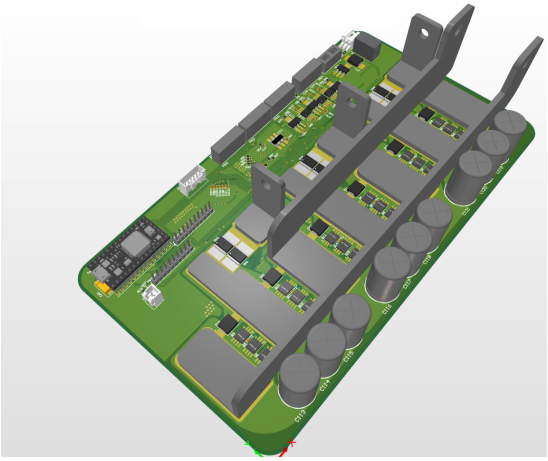

(a) Board design's first iteration.

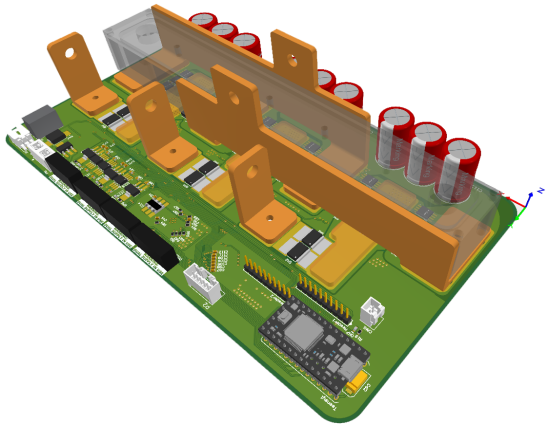

(b) The final PCB layout with new Busbar designs.

Figure 14: The controller's PCB.

IV.E. Heat sink design.

A heat sink had to be custom made for this application, since even though several standard PCB-Air heat sinks exist on the market, very few PCB-Liquid standard ones exist commercially, with most of them being dedicated to single ICs. Since this controller is meant to be manufactured in small quantities, it's important that the heat sink is easily manufactured with simple machining operations, thus making it's manufacture on IST possible.

The design process started with aluminium square stock, in which channels were cut, as well as a recess for a lid to fit into, leaving grooves for sealing O-rings to prevent coolant leakage on the islands between the channels. The bottom had most of it's surface machined, so as to leave small protrusions that make up the height difference between the busbars and the transistors, thus improving the thermal path through the MOSFETs' casings. Afterwards, a lid was designed out of $5mm$ aluminium flat stock, with a protrusion that fits inside the core, surrounded by an O-ring groove that seals the interface. These parts are screwed together with 9 M3 bolts, and screwed to the PCB with another 9 M3 bolts. A Sil-Pad will be needed to electrically isolate the busbars from the heat sink, and holes have been made in them to allow for an insulating nylon spacer to be fitted, along with the removal of the PCB copper surrounding the bolt holes, so as to prevent any electrical connection to the bolts which could cause a short-circuit.

A CFD analysis was performed, assuming an equally distributed $400W$ thermal load on the bottom surface and a $1l/min$ water flow, the design value for SR03's cooling system, and the design was iterated until the final version shown in figure 15. The water enters the core in the right side and flows through the channels, constantly hitting the walls and thus improving thermal transfer. When approaching the outlet, it hits a wall angled downwards, sending some of the cooler water on top to the bottom, providing additional cooling to the hottest part of the heat sink, near the outlet. It then flows around the wall thus staying longer and providing extra cooling, until leaving the heat sink.

The final results are promising, showing only a $15°C$ difference between the water temperature and the maximum temperature on the bottom of the heat sink (Figure 16). Note that, the input power is higher than the expected one, and in the edges there will be less heat flux, as they are only cooling down one triplet instead of 2 as in the middle, so this figure should, in practice, be lower.

IV.F. Lid Design.

With the hardware finalized, a concern about the proximity of the vertical portion of the busbars to the heat sink grew, as well as the possibility to rip them from the PCB due to leverage on the connection points and vibration. Finally, the exposed high power conductors were deemed as a serious electrical hazard, and thus a 3D printable plastic lid was designed to cover these important points, as well as to provide some mechanical rigidity to the busbars. It consists on 4 channels (Figure 17), one for the heat sink, surrounded by two, one for each battery busbar, and finally another one which cov-

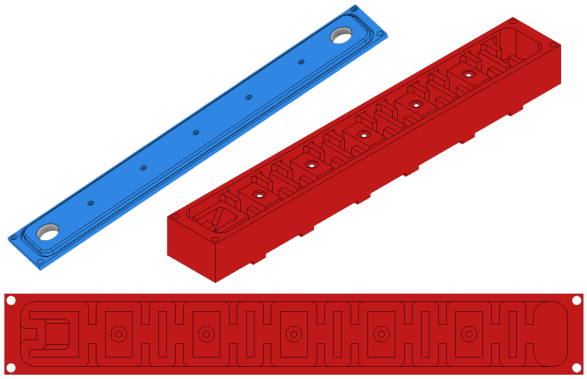

Figure 15: The designed heat sink, composed of a core (red) and a lid (blue).

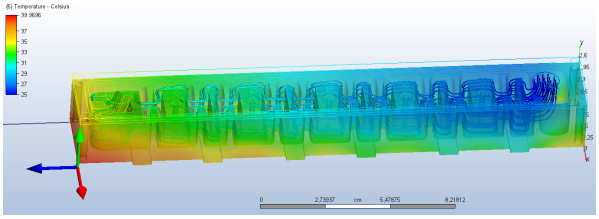

Figure 16: CFD analysis result.

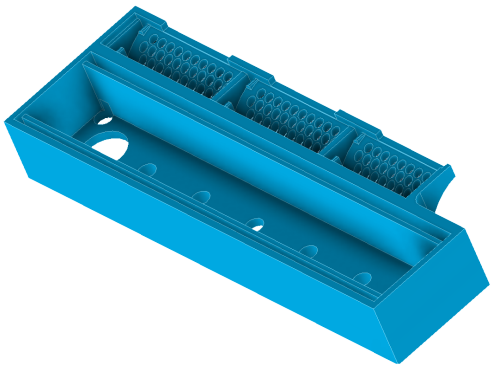

Figure 17: Lid's Lower view.

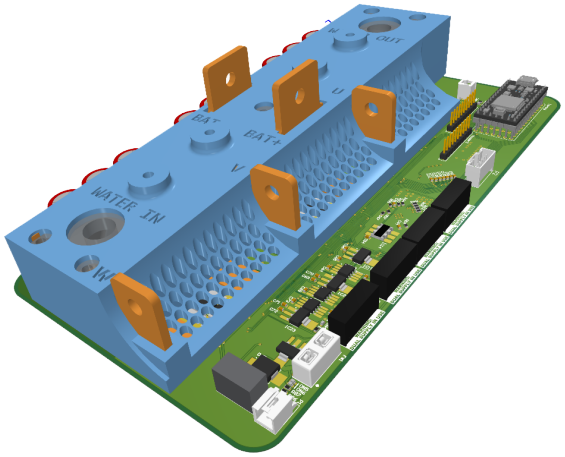

Figure 18: The final Motor Controller board.

ers the shunts, complete with ventilation holes and an air intake on the bottom, and supports the motor winding busbars. It will be attached using 4 of the heat sink's bolts, which shall be replaced with studs and nylon lock nuts, leaving some exposed thread for an extra nut which holds down the lid. Since the lid will be visible, some text was embossed in order to label the connections, which shall help with installation. The final result is depicted in Figure 18.

V. Conclusions

This master thesis led to the development of Técnico Solar Boat's own BLDC motor controller hardware, an important step to their goal of building in-house all of their boats' components. Plus, it's of simple construction, as the needed heat sink and copper busbars are of simple construction and can be fabricated in IST for a low cost. Besides, most of the main electronic components originate from the team's sponsors, leading to an inexpensive solution, easily implemented.

The final product is very compact, having a large power density, on par with any commercial solution. However, unlike the current commercial solution, the cooling should be capable of keeping the circuit operating at full power indefinitely, even inside an enclosed space, so the usable power output is significantly higher. Besides, it's behaviour is adjustable in several ways, controlling the MOSFET's turn on and turn off via resistances, ferrite beads and gate supply voltages, allowing several degrees of freedom for finding the ideal compromise between electrical noise and switching speed, and thus switching losses. Unlike the current commercial controller, this has galvanic isolation between the high power and control electronics, thus offering excellent protection against high power ground loops, which have previously dam-

aged several other controllers. This feature is especially useful for the controller's intended application, as it will be used on prototype boats, so the remaining system's hardware will be subject to frequent changes. Additionally, hardware based shoot-through protections are installed, which will prevent shorting out the half-bridges, something that could happen from faulty firmware or excessive electrical noise. Finally the logic side is protected from wrong polarity and overcurrents, making the developed controller well suited to prototyping, as it should be protected against the most common mistakes which could happen during it's usage.

Extra versatility was added with several external connection ports for additional hardware and sensors, which some control algorithms, or additional functions, may require. This, combined with the aforementioned hardware adjustments and powerful micro-controller, makes for a very capable test platform for motor control study, which will allow not only for the development of a motor control algorithm for the controller's intended usage, but also the testing of several others, as well as the behaviour of the MOSFET's under several conditions, thus becoming an important teaching tool.

REFERENCES

[1] Advanced Power Technology. *Eliminating Parasitic Oscillation between Parallel MOSFETs*, Março 2004.

[2] Analog Devices Inc, One Technology Way, P.O. Box 9106, Norwood, MA 02062-9106, U.S.A. *3.0 kV RMS, Single-Channel Digital Isolator*, Outubro 2015. Ficha Técnica: ADuM110N.

[3] Analog Devices Inc, One Technology Way, P.O. Box 9106, Norwood, MA 02062-9106, U.S.A. *Rail-to-Rail, Fast, Low Power 2.5 V to 5.5 V, Single-Supply TTL/CMOS Comparator*, Outubro 2015. Ficha Técnica: AD8468.

[4] Analog Devices Inc, One Technology Way, P.O. Box 9106, Norwood, MA 02062-9106, U.S.A. *16-Bit, Isolated, Sigma-Delta Modulator*, Agosto 2020. Ficha Técnica: ADuM7704.

[5] T. Ferreira. Projecto 5 - Motor e Controlador. Recrutamento TSB 2020, Outubro 2020.

[6] Infineon Technologies AG, Infineon Technologies AG 81726 Munich, Germany. *Isolated gate driving solutions Increasing power density and robustness with isolated gate driver ICs*, Março 2020.

[7] Infineon Technologies AG, Infineon Technologies AG 81726 Munich, Germany. *EiceDRIVER™ 1ED31xxMC12H Compact*, Março 2021. Ficha Técnica: 1ED3122MC12H.

[8] Infineon Technologies AG, Infineon Technologies AG 81726 Munich, Germany. *EiceDRIVER™ 2EDi product family - Fast, robust, dual-channel, functional and reinforced isolated MOSFET gate-driver with accurate and stable timing*, Abril 2021. Ficha Técnica: 2EDF7235K.

[9] Linear Technologies Inc, 1630 McCarthy Blvd., Milpitas, CA 95035-7417. *Multi-Sensor High Accuracy Digital Temperature Measurement System with EEPROM*, Janeiro 2016. Ficha Técnica: LTC2984.

[10] Texas Instruments Inc, Post Office Box 655303, Dallas, Texas 75265. *Quad Digital Filter for 2nd-Order Delta-Sigma Modulator*, Abril 2006. Ficha Técnica: AMC1210.

[11] Texas Instruments Inc, Post Office Box 655303, Dallas, Texas 75265. *DRV8302 Three Phase Gate Driver With Dual Current Shunt Amplifiers and Buck Regulator – Hardware Controlled*, Agosto 2011. Ficha Técnica: DRV8302.

[12] Texas Instruments Inc, Post Office Box 655303, Dallas, Texas 75265. *Isolated Shunt Current Measurement Reference Design With Standalone Digital Filters*, Agosto 2018.